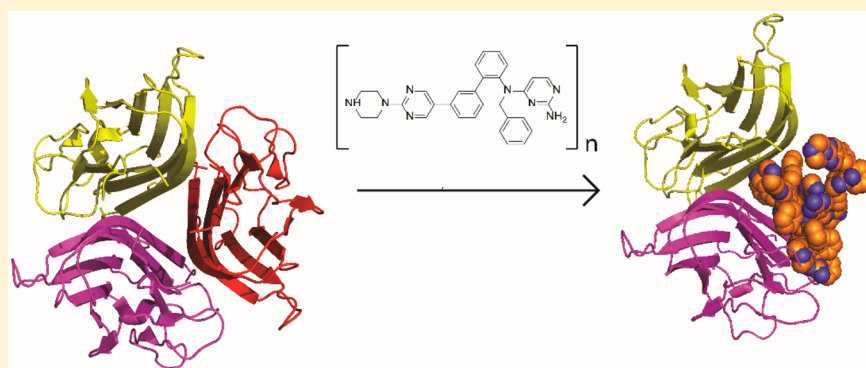


Structural Basis of Small-Molecule Aggregate Induced Inhibition of a Protein–Protein Interaction

Jonathan M. Blevitt,[†] Michael D. Hack,[‡] Krystal L. Herman,[†] Paul F. Jackson,[†] Paul J. Krawczuk,[§] Alec D. Lebsack,^{||} Annie X. Liu,[⊥] Taraneh Mirzadegan,[‡] Marina I. Nelen,[#] Aaron N. Patrick,[⊥] Stefan Steinbacher,[∇] Marcos E. Milla,^{†,○} and Kevin J. Lumb^{*,⊥,ⓑ}[†]Emerging Science & Innovation, Discovery Sciences, Janssen R&D LLC, La Jolla, California 92121, United States[‡]Lead Discovery, Discovery Sciences, Janssen R&D LLC, La Jolla, California 92121, United States[§]Immunology, Janssen R&D LLC, Spring House, Pennsylvania 19477, United States^{||}Immunology, Janssen R&D LLC, La Jolla, California 92121, United States[⊥]Emerging Science & Innovation, Discovery Sciences, Janssen R&D LLC, Spring House, Pennsylvania 19477, United States[#]Lead Discovery, Discovery Sciences, Janssen R&D LLC, Spring House, Pennsylvania 19477, United States[∇]Proteros Biostructures, 82152 Martinsried, Germany

S Supporting Information



ABSTRACT: A prevalent observation in high-throughput screening and drug discovery programs is the inhibition of protein function by small-molecule compound aggregation. Here, we present the X-ray structural description of aggregation-based inhibition of a protein–protein interaction involving tumor necrosis factor α (TNF α). An ordered conglomerate of an aggregating small-molecule inhibitor (JNJ525) induces a quaternary structure switch of TNF α that inhibits the protein–protein interaction between TNF α and TNF α receptors. SPD-304 may employ a similar mechanism of inhibition.

■ INTRODUCTION

Protein–protein interactions mediate numerous biological processes and provide a potential opportunity for the therapeutic interception and modulation of disease.¹ Therapeutic “large-molecule” antibodies provide an established approach to modulate extracellular protein–protein interactions. However, the ability to modulate protein–protein interactions with small molecules is much less developed than for traditional drug targets such as kinases, proteases, and G-protein coupled receptors. Nonetheless, progress has been made with attention focused on the identification of hot spots at protein–protein interfaces as avenues to identify inhibitors of protein–protein interactions.¹

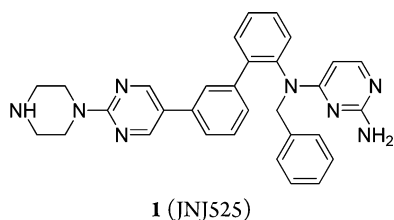
One approach to the discovery of small-molecule therapeutics is the identification of chemical starting points for optimization to drugs via high-throughput screening of compound libraries. However, screening of compound libraries

can return false positives that apparently modulate the target but do so in a way unrelated to an actual or relevant mechanism of action.² A common source of false positives is compound aggregation, which has been described to date in the context of enzymes and G-protein-coupled receptors.^{2a,3} In one study, 95% of active compounds from a high-throughput screen were aggregation-based inhibitors.⁴ In another study, 19% of randomly selected druglike compounds formed aggregates.⁵ Aggregates are proposed to form large assemblies that sequester proteins, perhaps as many as 10^4 enzyme molecules per aggregation particle, rather than acting as direct inhibitors² and may partially denature enzymes.⁶ Aggregation-induced inhibition can be insidious to drug discovery activities with examples of the optimization of structure–activity relationships that

Received: December 14, 2016

reflect aggregation-induced enzyme inactivation rather than active-site inhibition.⁷

Here we describe a compound-aggregation mechanism for a protein–protein interaction inhibitor. TNF α is a homotrimeric cytokine that binds two receptors, TNFR1 (also called CD120a) and TNFR2 (also called CD120b).⁸ Engagement of TNF α with TNFR1 and TNFR2 initiates signaling cascades that result in inflammatory responses and control of apoptosis.⁸ TNF α is the therapeutic target for five biologic drugs for the treatment of multiple autoimmune and inflammatory conditions, and TNF α -mediated pathways are also the target for small-molecule therapies for cancer.⁸ The biaryl substituted pyrimidine **1** (JNJ525), disclosed here, is an apparent small-molecule inhibitor of TNF α . However, **1** forms an aggregate that induces a quaternary structure change in TNF α . Thus, **1** inhibits protein function via an aggregation-based mechanism that is distinct from protein sequestration and denaturation mechanisms proposed for enzymes.^{2,6}



RESULTS AND DISCUSSION

The formation of complexes of the soluble form of TNF α with the soluble ectodomains of TNFR1 and TNFR2 can be monitored with TR-FRET between donor (Tb) and acceptor (d2) fluorophore pairs on TNF α and the receptor, respectively. Etanercept, a fusion protein of TNFR2 and a IgG1 heavy chain,⁹ inhibits the association of soluble TNF α with the ectodomains of TNFR1 and TNFR2, as expected,⁹ with apparent IC₅₀ values for both receptors of 12 \pm 1 pM (Figure 1A). These apparent IC₅₀ values are in accord with previously reported K_d of 11 pM for both receptors measured with SPR.¹⁰

Compound **1** also prevents the formation of TNF α complexes with TNFR1 and TNFR2. In the TR-FRET assay, the apparent IC₅₀ values for the inhibition of complex formation are 1.2 \pm 0.2 μ M and 1.1 \pm 0.1 μ M for TNFR1 and TNFR2, respectively (Figure 1A). Compound **1** does not cause a concentration-dependent decrease in signal in a TR-FRET technology artifact assay employing a protein–protein complex formed by antibodies labeled with the same fluorescent donor and acceptor pairs, suggesting that the observed inhibition is not a fluorescence artifact (Figure 2).

A hallmark of aggregation-induced inhibition of enzymes is the abrogation of inhibition by detergent, demonstrated most frequently with Triton X-100.^{4,5,11} Inhibition by etanercept of the TNF α complex with TNFR1 and TNFR2 is readily monitored in the presence of Triton X-100 even though addition of the detergent reduces the assay window (Figure 1B). The apparent IC₅₀ values for etanercept-mediated inhibition in the presence of Triton X-100 for TNF α complex formation with TNFR1 and TNFR2 are within 3-fold of the values in the absence of detergent at 9 \pm 1 pM and 5 \pm 1 pM, respectively (Figure 1B). In contrast, Triton X-100 abrogates the ability of **1** to inhibit the formation of TNF α complexes

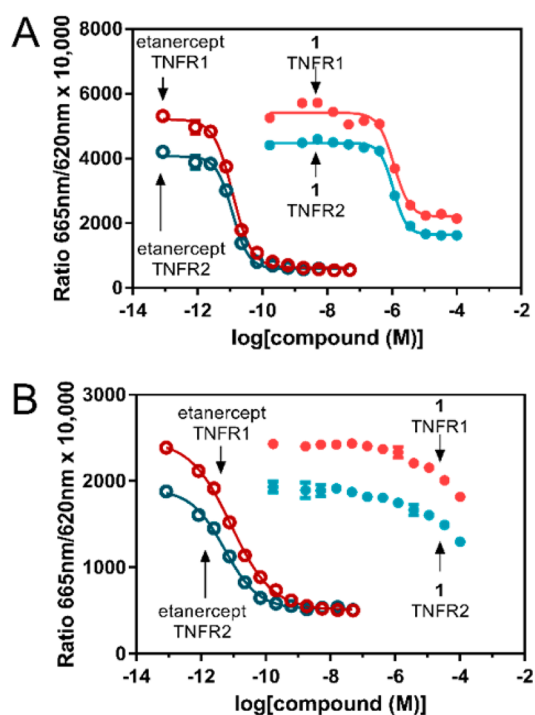


Figure 1. (A) Inhibition of the TNF α interaction with TNFR1 and TNFR2 monitored with TR-FRET by etanercept and **1**. The Hill slopes for TNFR1 and TNFR2 inhibition by **1** are 1.9 and 2.5, respectively. (B) The IC₅₀ values for the inhibition by etanercept of TNF α interaction with TNFR1 and TNFR2 monitored with TR-FRET are largely unaffected by detergent (0.1% Triton X-100). In contrast, the inhibition activity of **1** is abrogated by detergent (0.1% Triton X-100).

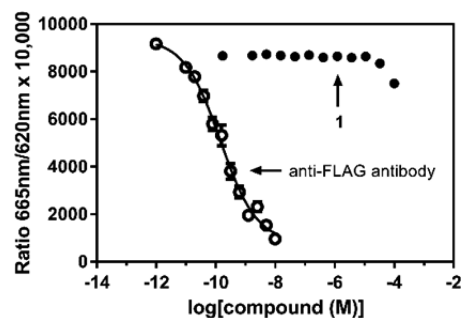


Figure 2. Compound **1** does not cause interference in the TR-FRET assay. The TR-FRET signal associated with a protein–protein interaction pair formed with Tb-labeled mouse anti-FLAG antibody and anti-mouse antibody labeled with the acceptor d2 is disrupted by titration with the unlabeled anti-FLAG antibody as expected and reflected in the loss of signal. Compound **1** does not cause a change in the TR-FRET signal at 10⁻⁵ M or below, indicating that **1** does not produce assay interference artifacts.

with TNFR1 and TNFR2, with a lack of a defined inhibition curve characterized by a meaningful IC₅₀ (Figure 1B).

The formation of an aggregate is characterized by the CAC, below which aggregate formation is low even in the presence of increasing concentration of the compound. At the CAC, aggregate formation increases sharply with compound concentration. Formation of aggregates can be monitored directly with techniques such as light scattering. In a high-throughput setting, optical biosensors provide an empirical measure of compound behavior that mimics aggregation. Such behavior was first

observed with SPR¹² and later with resonant waveguide grating.¹³ Miconazole, a known aggregator,¹⁴ gives a concentration-dependent profile monitored with resonant waveguide grating that is consistent with a CAC of 1 μ M (Figure 3).

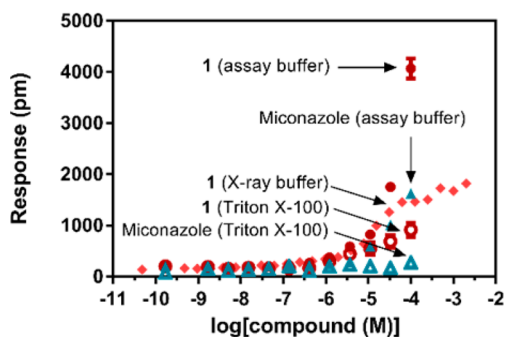


Figure 3. Compound 1 exhibits a concentration-dependent response as measured with an optical biosensor that is consistent with the formation of an aggregate with a CAC of 1 μ M in the biochemical assay (●) and crystallization (◆) buffers. Miconazole, a known aggregator,¹⁴ exhibits the concentration-dependent behavior expected of an aggregator (▲) that is abrogated with 0.1% Triton X-100 (○).

Detergent (Triton X-100) abrogates the aggregation behavior of miconazole (Figure 3). Compound 1 also exhibits a response consistent with a CAC of 1 μ M that is abrogated by Triton X-100 (Figure 3), in accord with the detergent effect on TR-FRET (Figure 1B). The monitoring of compound aggregation is not always unambiguous given that optical biosensing is an empirical approach, aggregation is sensitive to solution conditions, and aggregation may be modulated by the presence of protein. However, the coincidence of the CAC and IC₅₀ values and the detergent sensitivity suggest that the apparent inhibition observed in TR-FRET is consistent with an aggregate-induced phenomenon.

Analytical ultracentrifugation was used to characterize the oligomerization state of the TNF α complex with 1 using the $g(s)$ sedimentation velocity method.¹⁵ TNF α has a $s_{20,w}$ of 3.35 \pm 0.01 and a mass of 51.2 \pm 0.56 kDa with a $g(s)$ distribution that is accounted for with a single-species model. The observed mass is within the expected error of analytical ultracentrifugation (3–5%) of the expected value of the trimer (51 761 Da), in accord with previous analytical ultracentrifugation studies.¹⁶ In contrast, TNF α in the presence of 1 exhibits a $s_{20,w}$ of 3.09 \pm 0.04 and a mass of 41.3 \pm 1.2 kDa with a $g(s)$ distribution that is accounted for by a single-species model (Figure 4). The observed mass is consistent with TNF α forming a dimer in solution that is associated with approximately 13 molecules of 1 (the masses of the TNF α dimer and 1 are 34 507 Da and 514.6 Da, respectively).

The X-ray structure of TNF α bound to 1 was determined at 3.0 Å.¹⁷ The aggregation of 1, monitored with resonant waveguide grating detection, is also observed in the crystallization buffer (Figure 3). The soluble domain of TNF α crystallizes as a trimer, in the apo state and when bound to the ectodomain of TNFR2 (Figure 5A).¹⁸ In contrast, in the presence of 1, TNF α undergoes a quaternary structure change in which a conglomerate of 1 replaces one of the three TNF α subunits of the apo form (Figure 5B). While TNF α crystallizes as a dimer of dimers (Supporting Information Figure 1), the quaternary structure shown in Figure 5B is consistent with the mass of TNF α in solution (Figure 4).

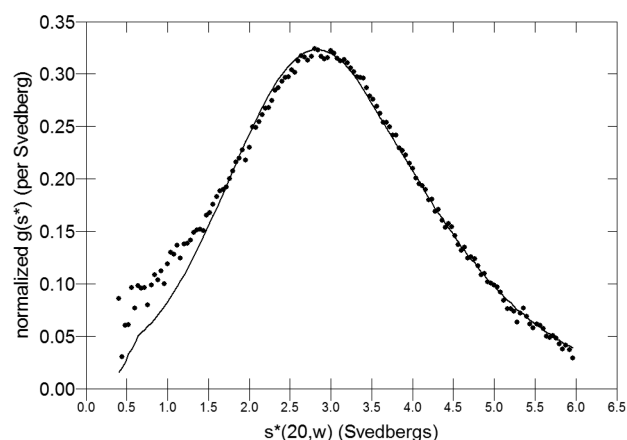


Figure 4. The sedimentation velocity $g(s)$ profile is accounted for by a single-species model at s values above 1.5. Reproducible deviation is seen at s values below 1.5, presumably reflecting an absorbance contribution from 1 that is different in the reference buffer and in the presence of TNF α .

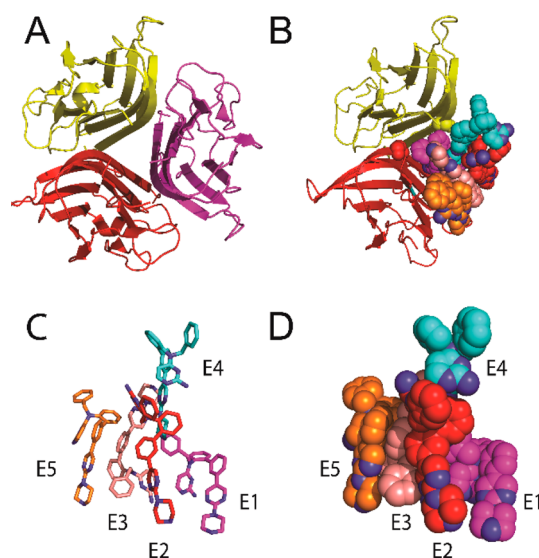


Figure 5. (A) The soluble domain of TNF α forms a homotrimer (yellow, red, and magenta) in the crystal structure.¹⁸ (B) Crystal structure of the complex formed by the soluble domain of TNF α with 1 (orange with N atoms in blue), in which the aggregate formed by 1 displaces one of the TNF α subunits. The conformations of the subunits of the TNF α –1 complex are similar to that of apo TNF α (PDB code 1TNF) with a C $_{\alpha}$ rmsd of 0.8 Å for chains A and B of both structures. (C) Conglomerate of 1 comprising ligands E1–E5. The C atoms of each molecule are shown in a different color with N atoms shown in blue. (D) Space-filling representation of the conglomerate of 1, colored as in part C.

In the crystal structure, TNF α binds a conglomerate formed by five molecules of 1 (Figure 5B). A sixth ligand shows only partial density and has not been included. The ligand conglomerate is nonsymmetric, and all ligands show different contacts to the protein or other ligands (Figure 5C), which precludes a straightforward evaluation of structure–activity relationships for TNF α binding and aggregation.

Ligands E1 and E2 participate in protein–ligand contacts, whereas E3–E5 engage primarily in hydrophobic ligand to ligand contacts. Ligand E1 forms three hydrogen bonds with TNF α chain A that involve Ser 60 CO, Leu 120 CO and Tyr

151 OH (Figure 6). The interactions within the ligand conglomerate are exclusively hydrophobic, and neither the

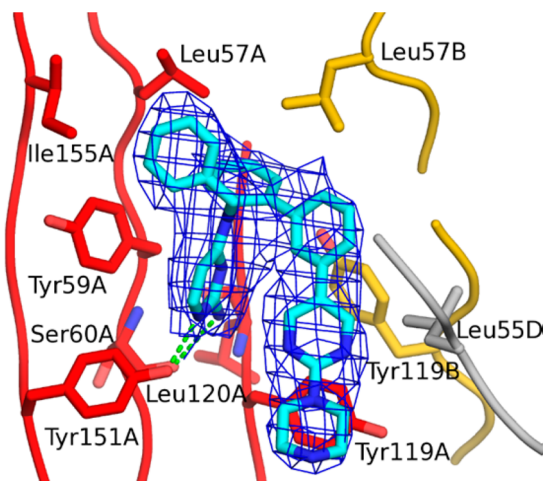


Figure 6. Ligand E1 of the aggregate formed by **1** and neighboring protein side chains (**1** in cyan, TNF α chains A, B, and D in red, yellow, and gray, respectively, N in blue and O in red). Hydrogen bonds are shown as green dotted lines. The ligand molecule is shown superimposed with the refined $2F_o - F_c$ electron density map contoured at 1.0σ . Ligand E1 forms three hydrogen bonds with TNF α chain A that involve Ser 60 CO, Leu 120 CO, and Tyr 151 OH. All atoms involved in these hydrogen bonds are well-defined by the electron density. Other residues of chain A in the vicinity of the ligand E1 (within 3.9 Å) are Leu 57, Tyr 59, Ser 60, Tyr 119, Leu 120, Tyr 151, and Ile 155. The binding pocket is completed by Leu 57 and Tyr 119 of chain B and Leu 55 of chain D. In addition to the interactions shown for ligand E1, ligand E2 binds close to protein chains C and D. Tyr 151 OH (chain D) forms an H-bond with the ligand, whereas the remaining interactions are hydrophobic in nature. These involve in chain C Leu 57, Tyr 59, Ile 155, Leu 157 and in chain D Lys 11, Leu 57, Tyr 59, Ile 155, Leu 157. Ligand E3 also forms an H-bond to Tyr 151 OH (chain A) with its amino group and a smaller number of hydrophobic contacts to three subunits (chain A, His 15, Tyr 59, Ile 155; chain B, Leu 157; chain C, Val 13, Ile 155). Ligand E4 participates only in a few hydrophobic contacts to the protein (chain B, Leu 55, Leu 157; chain C, Tyr 119; chain D, Tyr 119). The amino group of the ligand and Tyr 151 OH are too far apart for hydrogen bonding. Ligand E5 binds between chains A and C via hydrophobic contacts with TNF α (chain A, Ser 9, Lys 11, Val 13, Leu 36, Ile 155; chain C, Val 13, His 15, Leu 36, Tyr59). The amino group of E5 points toward the solvent.

piperazine nor the amino group of the ligands engages in interligand contacts (Figure 5D).

Compound **2** (SPD-304)¹⁹ is a small-molecule inhibitor of TNF α that is described as favoring a dimeric form of TNF α .¹⁹ The TNF α structure induced by **2** is very similar to that induced by **1** (Supporting Information Figure 1). The apparent IC₅₀ values for the inhibition of TNF α binding to TNFR1 and TNFR2 are 1.3 and 1.2 μ M, respectively (Supporting Information Figure 2A), and inhibition is abrogated by detergent (Supporting Information Figure 2B). Moreover, **2** forms an aggregate with a CAC of 10 μ M (Supporting Information Figure 2C). Thus, **2** appears to inhibit TNF α via an aggregate-induced mechanism. In the crystal structure of TNF α with **2**, one molecule of **2** was modeled per TNF α dimer.¹⁹ However, the crystal structure contains unexplained electron density that could reflect a aggregate of **2** analogous to that seen for **1** (Supporting Information Figure 3). It is possible

that **2** employs the same aggregation-induced mechanism of TNF α quaternary structure rearrangement as exhibited by **1**. It is noted that although **2** is reported to exhibit cell-based activity,¹⁹ **2** is toxic to cells (Supporting Information Figure 4).

Aggregator Advisor is a tool that identifies molecules that are known to aggregate or may aggregate based on chemical similarity to known aggregators.²⁰ Neither **1** nor **2** is similar to the aggregators in the Aggregation Advisor database, although the cLogP of 5.9 of **1** and 6.4 of **2** is consistent with properties of known aggregators.

CONCLUSION

The mechanism of aggregation-induced inhibition of enzymes has been described as a multistep process. First, the aggregating molecule adopts a large colloid of approximately 30–600 nm in size.²¹ Second, the colloid sequesters the enzyme with potentially 10⁴ molecules of enzyme per particle.¹⁴ Finally, the enzyme may be destabilized or partially denatured on binding the aggregate.⁶

In contrast to mechanisms described for enzymes,^{6,14,21} **1** forms an aggregating conglomerate that competes for a protein subunit of the TNF α trimer and induces a change in quaternary structure. TNF α receptor binding is disrupted upon the quaternary structure rearrangement induced by the aggregate.

The finding illustrates a mechanism of action for protein–protein interactions via disruption of quaternary structure via a small-molecule conglomerate in addition to allosteric occupancy of hot spots at protein–protein interfaces. It is conceivable that small molecules can cause quaternary structure changes in a range of proteins involved in catalysis and protein–protein interactions that regulate a range of processes.

EXPERIMENTAL METHODS

Synthesis of Compound 1. The five-step synthetic scheme is described in the Supporting Information. The final step is Boc deprotection. *tert*-Butyl 4-(5-(2'-((2-aminopyrimidin-4-yl)(benzyl)amino)[1,1'-biphenyl]-3-yl)pyrimidin-2-yl)piperazine-1-carboxylate (0.09 g, 0.15 mmol) was dissolved in DCM (2.4 mL), and TFA (0.4 mL, 5.3 mmol) was added at room temperature. The mixture was stirred for 30 min, after which LCMS and TLC showed consumption of the starting material. The reaction solution was concentrated to dryness and azeotroped thrice with DCM (3 mL), to remove residual TFA, and dried under vacuum. The crude material was then purified with reversed phase HPLC using a Luna C18 (5 μ m particle size, 100 mm \times 30 mm) column (Phenomenex) using a 10–90% gradient of acetonitrile in water containing 0.1% TFA. The fractions containing the product were lyophilized to provide the product as a white powder (0.07 g, 75% yield). The purity is >99% as assessed by C₁₈ HPLC using a water/acetonitrile gradient containing 0.1% TFA monitored at 245 and 280 nm. The expected structure of **1** is consistent with the X-ray structure of **1** in the complex with TNF α (Figure 6). ESI-TOF mass spectrometry: m/z : [M + H]⁺ calculated 515.2672; found 515.2678. ¹H NMR (400 MHz, methanol-*d*₄): δ 8.62 (s, 2H), 7.65 (d, J = 7.4 Hz, 1H), 7.63–7.60 (m, 2H), 7.59–7.54 (m, 1H), 7.54–7.48 (m, 1H), 7.44–7.37 (m, 2H), 7.30–7.25 (m, 1H), 7.23–7.19 (m, 3H), 7.18–7.13 (m, 2H), 7.04–6.98 (m, 1H), 5.95 (d, J = 7.4 Hz, 1H), 5.60 (d, J = 14.4 Hz, 1H), 4.17–4.07 (m, 5H), 3.33–3.31 (m, 4H). ¹³C NMR (151 MHz, CD₃OD): δ 163.88, 160.41, 160.10, 155.81, 150.23, 139.90, 139.57, 138.78, 136.78, 135.23, 131.53, 130.15, 129.28, 128.75, 128.43, 127.94, 127.46, 127.07, 125.76, 125.00, 123.85, 117.79, 115.85, 96.05, 51.76, 43.20, 41.02.

Proteins. The soluble domain of human TNF α (residues 77–233) was expressed and purified at Proteros Biostructures (Martinsried, Germany). Etanercept was obtained from Caligro Rx, Inc., (Dartford, U.K.). The extracellular domains of human TNFR1 (residues 22–211; Sino Biologics 10872-H08H) and human TNFR2 (residues 23–257;

Sino Biologicals 10417-H08H) expressed in human cells were directly labeled with the TR-FRET acceptor d2 by random conjugation of primary amines at Cisbio Bioassays (Bedford, MA).

Tb-Labeled TNF α . The soluble domain of human TNF α (residues 77–233) with the mutation T83C (TNF α -T83C) and a N-terminal His₆-tag followed by a TEV protease cleavage site was expressed in *Escherichia coli* strain BL21 (DE3). Protein expression in *Escherichia coli* strain BL21 (DE3) was induced with 0.2 mM IPTG at 16 °C overnight (18–22 h). Cells were harvested with centrifugation and stored at –80 °C before purification. Cells were lysed with a microfluidizer in 20 mM Tris-HCl, pH 8.0, 500 mM NaCl, 20 mM imidazole, pH 8.0, 7 mM β ME and purified with Ni-affinity chromatography. The target protein was eluted with a 10 column-volume gradient of 20–300 mM imidazole. The His₆-tag was removed with TurboTEV protease (1:50 TEV:TNF α) and the target protein passed over Ni-affinity chromatography. The flow through was further purified by anion exchange chromatography using a HiTrap Q HP and eluted with a 10 column-volume gradient of 50–500 mM NaCl. Peak fractions were dialyzed overnight against 10.01 mM Na₂HPO₄, 1.76 mM KH₂PO₄, 136.9 mM NaCl, 2.68 mM KCl, pH 7.4 (Corning Cellgro 46-013-CM), concentrated, passed through a 0.2 μ m filter, aliquoted, and frozen. The identity of the protein was verified by N-terminal sequencing and mass spectrometry. The protein was directly labeled using Lumi4-Tb-maleimide (Cisbio 60MISZZZ). 0.1 mM TNF α -T83C was incubated with 0.4 mM Lumi4-Tb-maleimide and 0.2 mM TCEP (ThermoFisher 77720B) for 2 h at room temperature in 5.6 mM Na₂HPO₄, 1 mM KH₂PO₄, and 154 mM NaCl, pH 7.4 (Corning 21-040-CV). The Tb-labeled product was purified from unincorporated label using a Superdex 200 Increase size-exclusion column (GE 28990944) equilibrated in 5.6 mM Na₂HPO₄, 1 mM KH₂PO₄, and 154 mM NaCl, pH 7.4 (Corning 21-040-CV).

TR-FRET. Assays were performed with a PHERAStar FS (BMG Labtech) in 1536-well white, nontreated flat bottom plates (Corning 3725) in a final volume of 4 μ L in 5.6 mM Na₂HPO₄, 1 mM KH₂PO₄, and 154 mM NaCl, pH 7.4 (Corning 21-040-CV), containing 0.01% casein (G-Biosciences 786-194) and 1% DMSO at room temperature. In some cases, 0.1% Triton X-100 (Thermo Scientific 85111) was included in the assay buffer. Assays contained 0.25 nM Tb-labeled TNF α and 0.5 nM d2-labeled TNRF1 or 0.25 nM Tb-labeled TNF α and 4 nM d2-labeled TNRF2. TR-FRET was measured with a 60 μ s delay after the excitation pulse and a 400 μ s read time with excitation at 337 nm. Emission was measured at 620 and 665 nm. Results are expressed as the ratio of fluorescence intensities at 665 nm and 620 nm \times 10 000. Compound was incubated with TNF α for 1 h prior to addition of the receptor and incubated for a further 2 h before the read. The technology artifact assay was performed as described above except 0.1 nM Tb-labeled anti-FLAG antibody raised in mice (Cisbio 61FG2TLA) and 0.2 nM d2-labeled anti-mouse IgG raised in rabbits (Cisbio 61PAMDAA) were used to generate the protein–protein pair. The titrated antibody is unlabeled anti-FLAG raised in mice (Sigma F1804).

Compound Aggregation. Optical sensor assays of compound behavior were performed with EPIC (Corning) in 384-well plates (Corning 5040) in the TR-HTRF assay buffer (vide supra) or crystallization buffer (vide infra) at room temperature. Miconazole (Sigma M3512) was used as a positive control for compound aggregation. Plates were equilibrated for 1.5 h in 50 μ L of assay buffer for the baseline read prior to compound addition (0.5 μ L) and incubated for 30 min prior to the final read.

Analytical Ultracentrifugation. Sedimentation velocity data were collected at 20 °C with a Beckman XL-I. Samples were dialyzed against 5.6 mM Na₂HPO₄, 1 mM KH₂PO₄, and 154 mM NaCl, pH 7.4 (Corning 21-040-CV). Samples of 10 μ M TNF α or the reference buffer alone were prepared from a single solution of the dialysate containing 50 μ M **1** with DMSO present at a concentration of 1% (the visual solubility limit of **1** in the study buffer is >50 μ M but <100 μ M). Samples were incubated for 3 h, with at least 1 h in the ultracentrifuge at 20 °C, prior to data collection. One scan at 280 nm was collected at 50 krpm in continuous mode. Sedimentation velocity data were analyzed with the g(s) method using DCDC+ version 2.4.3.^{15,22}

Structure Determination. The protein was prepared at 48 mg/mL in 10 mM Tris-HCl, pH 7.5 (Sigma T4661), and 50 mM NaCl (Sigma 71376) and mixed with 100 mM **1** in DMSO (the final concentration of **1** was 3.3 mM). TNF α and **1** were incubated for 30 min prior to mixing 1:1 with the reservoir solution comprising 0.01 M sodium acetate, pH 4.60 (Sigma 71188), 0.24 M sodium malonate (Sigma M1875), 9% (w/v) PEG3350 (Sigma 88276), 0.05 M sodium citrate, pH 6.00 (Sigma 71402), and 0.1069 M NaCl (Sigma 71376). Crystals were grown using sitting-drop vapor diffusion at 20 °C. Crystals appeared after 2 days and harvested after 16 days. For cryocrystallography 1 M trimethylamine *N*-oxide was added using the Picodropper technology.²³ X-ray diffraction data were collected with the Swiss Light Source beamline PXI-X06SA. Data were processed using XDS and XSCALE.²⁴ Phase information was obtained by molecular replacement with Phaser²⁵ using initially a dimer of TNF α from a nonsymmetric trimer solved previously. Initial molecular replacement solutions indicated the presence of dimer of dimers which were used in a second run to place all molecules. Model building and refinement were performed with COOT and REFMACS.²⁶ TLS refinement was performed with REFMACS.²⁷ The ligand parametrization and generation of the corresponding library files were performed with CORINA.²⁸ The water model was built with the “Find waters” algorithm of COOT^{26b} by placing water molecules in peaks of the $F_o - F_c$ map contoured at 3.0σ followed by refinement with REFMACS and checking all waters with the validation tool of COOT.^{26b} The criteria for the list of suspicious waters were *B* factor greater than 80 Å², $2F_o - F_c$ map less than 1.2σ , distance to closest contact of <2.3 Å or >3.5 Å. The suspicious water molecules and those in the ligand binding site (distance to ligand less than 10 Å) were inspected manually. Up to 5 molecules of **1** were modeled per dimer of dimers. A sixth ligand molecule is partially disordered in some instances and was not included in the final model.

Cell-Based Assays. Normal human dermal fibroblasts cells (Lonza CC-2511) were plated at a density of 5000 cells/well in 40 μ L of complete media (Lonza CC-3131) in 384-well clear-bottom black-well plates (Corning 3712) and incubated overnight at 37 °C in the presence of 5% CO₂. Compounds were incubated with TNF α (1 ng/mL final concentration, R&D Systems 210-TA-020/CF) for 1 h in a 1:1 mix of serum-free media and complete media, added to cells, and incubated for 6 h at 37 °C in the presence of 5% CO₂. Supernatant was used for an IL6 immunoassay performed per the manufacturer's instructions (PerkinElmer AL223F). Cell viability was quantified with ATP-monitoring luminescence performed per the manufacturer's instructions (PerkinElmer 6016941).

■ ASSOCIATED CONTENT

📄 Supporting Information

The Supporting Information is available free of charge on the ACS Publications website at DOI: 10.1021/acs.jmedchem.6b01836.

Synthetic methods, structure determination statistics, and experimental data for **2** (PDF)

Accession Codes

Atomic coordinates have been deposited in the Protein Data Bank (PDB code 5MU8).

■ AUTHOR INFORMATION

Corresponding Author

*E-mail: klumb@its.jnj.com. Telephone: 215-628-5801.

ORCID

Kevin J. Lumb: 0000-0003-2778-9956

Present Address

○M.E.M.: Adaptive Biotechnologies, San Diego, California, United States.

Notes

The authors declare the following competing financial interest(s): The authors are or were employees of the Janssen Pharmaceuticals Companies of Johnson & Johnson and may hold stock in Johnson & Johnson.

ACKNOWLEDGMENTS

The authors thank C. Schalk-Hihi for oversight of protein production of TNF α -T83C at an external contract-research organization. The study was funded by Janssen Research & Development, LLC.

ABBREVIATIONS USED

CAC, critical aggregation concentration; DCM, dichloromethane; DMSO, dimethyl sulfoxide; ESI-TOF, electrospray ionization time-of-flight; HPLC, high-performance liquid chromatography; LCMS, liquid chromatography–mass spectrometry; NMR, nuclear magnetic resonance; SPR, surface-plasmon resonance; TFA, trifluoroacetic acid; TLC, thin-layer chromatography; TNF α , tumor necrosis factor α ; TNFR1, tumor necrosis factor receptor 1; TNFR2, tumor necrosis factor receptor 2; TR-FRET, time-resolved fluorescent resonance energy transfer; rmsd, root-mean-square deviation

REFERENCES

- (1) Arkin, M. R.; Tang, Y.; Wells, J. A. Small-molecule inhibitors of protein-protein interactions: Progressing toward the reality. *Chem. Biol.* **2014**, *21*, 1102–1114.
- (2) (a) Shoichet, B. K. Screening in a spirit haunted world. *Drug Discovery Today* **2006**, *11*, 607–615. (b) Thorne, N.; Auld, D. S.; Ingles, J. Apparent activity in high-throughput screening: Origins of compound-dependent assay interference. *Curr. Opin. Chem. Biol.* **2010**, *14*, 315–324.
- (3) Sassano, M. F.; Doak, A. K.; Roth, B. L.; Shoichet, B. K. Colloidal aggregation causes inhibition of G protein-coupled receptors. *J. Med. Chem.* **2013**, *56*, 2406–2414.
- (4) Feng, B. Y.; Simeonov, A.; Jadhav, A.; Babaoglu, K.; Ingles, J.; Shoichet, B. K.; Austin, C. P. A high-throughput screen for aggregation-based inhibition in a large compound library. *J. Med. Chem.* **2007**, *50*, 2385–2890.
- (5) Feng, B. Y.; Shelat, A.; Doman, T. N.; Guy, R. K.; Shoichet, B. K. High-throughput assays for promiscuous inhibitors. *Nat. Chem. Biol.* **2005**, *1*, 146–148.
- (6) Coan, K. E.; Maltby, D. A.; Burlingame, A. L.; Shoichet, B. K. Promiscuous aggregate-based inhibitors promote enzyme unfolding. *J. Med. Chem.* **2009**, *52*, 2067–2075.
- (7) Ferreira, R. S.; Bryant, C.; Ang, K. K.; McKerrow, J. H.; Shoichet, B. K.; Renslo, A. R. Divergent modes of enzyme inhibition in a homologous structure-activity series. *J. Med. Chem.* **2009**, *52*, 5005–5008.
- (8) Brenner, D.; Blaser, H.; Mak, T. W. Regulation of tumour necrosis factor signalling: Live or let die. *Nat. Rev. Immunol.* **2015**, *15*, 362–374.
- (9) Peppel, K.; Crawford, D.; Beutler, B. A tumor necrosis factor (TNF) receptor-IgG heavy chain chimeric protein as a bivalent antagonist of TNF activity. *J. Exp. Med.* **1991**, *174*, 1483–1489.
- (10) Shealy, D. J.; Cai, A.; Staquet, K.; Baker, A.; Lacy, E. R.; Johns, L.; Vafa, O.; Gunn, G., 3rd; Tam, S.; Sague, S.; Wang, D.; Brigham-Burke, M.; Dalmonte, P.; Emmell, E.; Pikounis, B.; Bugelski, P. J.; Zhou, H.; Scallon, B. J.; Giles-Komar, J. Characterization of golimumab, a human monoclonal antibody specific for human tumor necrosis factor alpha. *mAbs* **2010**, *2*, 428–439.
- (11) (a) Feng, B. Y.; Shoichet, B. K. A detergent-based assay for the detection of promiscuous inhibitors. *Nat. Protoc.* **2006**, *1*, 550–553. (b) Jadhav, A.; Ferreira, R. S.; Klumpp, C.; Mott, B. T.; Austin, C. P.; Ingles, J.; Thomas, C. J.; Maloney, D. J.; Shoichet, B. K.; Simeonov, A.

Quantitative analyses of aggregation, autofluorescence, and reactivity artifacts in a screen for inhibitors of a thiol protease. *J. Med. Chem.* **2010**, *53*, 37–51. (c) McGovern, S. L.; Helfand, B. T.; Feng, B.; Shoichet, B. K. A specific mechanism of nonspecific inhibition. *J. Med. Chem.* **2003**, *46*, 4265–4272. (d) Ryan, A. J.; Gray, N. M.; Lowe, P. N.; Chung, C. W. Effect of detergent on "promiscuous" inhibitors. *J. Med. Chem.* **2003**, *46*, 3448–3451.

(12) Giannetti, A. M.; Koch, B. D.; Browner, M. F. Surface plasmon resonance based assay for the detection and characterization of promiscuous inhibitors. *J. Med. Chem.* **2008**, *51*, 574–580.

(13) Randle, D. H.; Krebs, K. A.; Gitschier, H. J.; Upton, T. M. Label-free detection of compound aggregation using Corning EPIC technology. www.corning.com/lifesciences, 2011 (accessed March 5, 2016).

(14) Coan, K. E.; Shoichet, B. K. Stoichiometry and physical chemistry of promiscuous aggregate-based inhibitors. *J. Am. Chem. Soc.* **2008**, *130*, 9606–9612.

(15) Stafford, W. F. Boundary analysis in sedimentation transport experiments: A procedure for obtaining sedimentation coefficient distributions using the time derivative of the concentration profile. *Anal. Biochem.* **1992**, *203*, 295–301.

(16) Wingfield, P.; Pain, R. H.; Craig, S. Tumour necrosis factor is a compact trimer. *FEBS Lett.* **1987**, *211*, 179–184.

(17) TNF α in the presence of **1** crystallized as a dimer of dimers (Supporting Information Figure 1). Refinement of the final X-ray derived model is good with R_{cryst} and R_{free} values of 21.1% and 30.0%, respectively (Supporting Information Table 1). The geometry and stereochemistry of the refined model are good with 81% of the residues in the most favored region of the Ramachandran plot, 17.5% in the additionally allowed region, and 0.9% in the generously allowed region (Supporting Information Table 1).

(18) (a) Eck, M. J.; Sprang, S. R. The structure of tumor necrosis factor- α at 2.6 Å resolution. Implications for receptor binding. *J. Biol. Chem.* **1989**, *264*, 17595–17605. (b) Mukai, Y.; Nakamura, T.; Yoshikawa, M.; Yoshioka, Y.; Tsunoda, S.; Nakagawa, S.; Yamagata, Y.; Tsutsumi, Y. Solution of the structure of the TNF-TNFR2 complex. *Sci. Signaling* **2010**, *3*, ra83.

(19) He, M. M.; Smith, A. S.; Oslob, J. D.; Flanagan, W. M.; Braisted, A. C.; Whitty, A.; Cancilla, M. T.; Wang, J.; Lugovskoy, A. A.; Yoburn, J. C.; Fung, A. D.; Farrington, G.; Eldredge, J. K.; Day, E. S.; Cruz, L. A.; Cachero, T. G.; Miller, S. K.; Friedman, J. E.; Choong, I. C.; Cunningham, B. C. Small-molecule inhibition of TNF- α . *Science* **2005**, *310*, 1022–1025. This publication discloses compound **2** (6,7-dimethyl-3-[[methyl[2-[methyl[[1-[3-(trifluoromethyl)phenyl]-1H-indol-3-yl]methyl]amino]ethyl]amino]methyl]-(4H-1-benzopyran-4-one dihydrochloride)).

(20) Irwin, J. J.; Duan, D.; Torosyan, H.; Doak, A. K.; Ziebart, K. T.; Sterling, T.; Tumanian, G.; Shoichet, B. K. An aggregation advisor for ligand discovery. *J. Med. Chem.* **2015**, *58*, 7076–7087.

(21) McGovern, S. L.; Caselli, E.; Grigorieff, N.; Shoichet, B. K. A common mechanism underlying promiscuous inhibitors from virtual and high-throughput screening. *J. Med. Chem.* **2002**, *45*, 1712–1722.

(22) Philo, J. S. Improved methods for fitting sedimentation coefficient distributions derived by time-derivative techniques. *Anal. Biochem.* **2006**, *354*, 238–246.

(23) Bottcher, J.; Jestel, A.; Kiefersauer, R.; Krapp, S.; Nagel, S.; Steinbacher, S.; Steuber, H. Key factors for successful generation of protein-fragment structures: Requirement on protein, crystals, and technology. *Methods Enzymol.* **2011**, *493*, 61–89.

(24) Kabsch, W. XDS. *Acta Crystallogr., Sect. D: Biol. Crystallogr.* **2010**, *66*, 125–132.

(25) McCoy, A. J.; Grosse-Kunstleve, R. W.; Adams, P. D.; Winn, M. D.; Storoni, L. C.; Read, R. J. Phaser crystallographic software. *J. Appl. Crystallogr.* **2007**, *40*, 658–674.

(26) (a) Winn, M. D.; Ballard, C. C.; Cowtan, K. D.; Dodson, E. J.; Emsley, P.; Evans, P. R.; Keegan, R. M.; Krissinel, E. B.; Leslie, A. G.; McCoy, A.; McNicholas, S. J.; Murshudov, G. N.; Pannu, N. S.; Potterton, E. A.; Powell, H. R.; Read, R. J.; Vagin, A.; Wilson, K. S. Overview of the CCP4 suite and current developments. *Acta*

Crystallogr., Sect. D: Biol. Crystallogr. **2011**, *67*, 235–242. (b) Emsley, P.; Lohkamp, B.; Scott, W. G.; Cowtan, K. Features and development of COOT. *Acta Crystallogr., Sect. D: Biol. Crystallogr.* **2010**, *66*, 486–501.

(27) Winn, M. D.; Murshudov, G. N.; Papiz, M. Z. Macromolecular TLS refinement in REFMAC at moderate resolutions. *Methods Enzymol.* **2003**, *374*, 300–321.

(28) Gasteiger, J.; Rudolph, C.; Sadowski, J. Automatic generation of 3D-atomic coordinates for organic molecules. *Tetrahedron Comput. Methodol.* **1990**, *3*, 537–547.